Molecular Crystals and Liquid Crystals Science and Technology. Section A. Molecular Crystals and Liquid Crystals

Publication details, including instructions for authors and subscription information:
http://www.tandfonline.com/loi/gmcl19

Classical and Quantum Mechanical Models for Stark Experiments

Bryan E. Kohler [a] & Jörg C. Woehl [a]

[a] Chemistry Department, University of California, Riverside, CA, 92521, USA

Version of record first published: 04 Oct 2006.

To cite this article: Bryan E. Kohler & Jörg C. Woehl (1996): Classical and Quantum Mechanical Models for Stark Experiments, Molecular Crystals and Liquid Crystals Science and Technology. Section A. Molecular Crystals and Liquid Crystals, 291:1, 119-134

To link to this article: http://dx.doi.org/10.1080/10587259608042739

Mol. Cryst. Liq. Cryst., 1996, Vol. 291, pp. 119–134
Reprints available directly from the publisher
Photocopying permitted by license only

CLASSICAL AND QUANTUM MECHANICAL MODELS FOR STARK EXPERIMENTS

BRYAN E. KOHLER AND JÖRG C. WOEHL
Chemistry Department, University of California, Riverside, CA 92521, USA

Abstract The resolution enhancement of photochemical hole burning makes it possible to directly see the effect that an external electric field has on the transition energy resolution of a probe molecule in an organic solid. With an appropriate interpretative model, these experiments can give a detailed picture of intermolecular electrostatic interaction. In this paper classical and quantum mechanical models are reviewed and applied to the same data set. We demonstrate that a relatively simple yet microscopically detailed and easily generalized quantum mechanical model can give an atomic resolution map of electrostatic potential at the chromophore site.

INTRODUCTION

The resolution enhancement that can be achieved by hole burning has made it possible to directly observe the effect that an external electric field has on the excitation energy of a probe molecule in a complex molecular solid. Even qualitative aspects of the response of a photochemical hole to external field convey significant information about local structure. For example, a field induced splitting of the hole for a sample where the probe molecules are randomly oriented in the laboratory frame implies significant local order and the magnitude of the splitting correlates with the strength of the effective internal electric field. While these kinds of qualitative considerations already significantly advance our ability to characterize local environment and intermolecular interaction, the full potential of these kinds of measurements, a *quantitative* microscopic mapping of electrostatic potential, requires a reasonable interpretative model. An ideal model would contain the correct fundamental physics in a form that is intuitively clear and easy to use and would give new insights into the structure of complex organic solids. This paper describes the evolution of our own ideas about the model that should be used. To make the content and limitations of each of the models more concrete, they are used to analyze Stark profiles measured for octatetraene in n-hexane and octatetraene in n-heptane.

Calculating Hole Profiles

Knowledge of the lineshape for the unperturbed probe molecule, the dependence of excitation energy on electric field or electrostatic potential, and the properties of the experimental ensemble is sufficient information for the calculation of a Stark profile. Given that the hole profile for the unperturbed molecule is one of the things that can be directly measured, it is best taken from experiment. As is the case for many other systems, the zero external field hole profiles for octatetraene in n-alkanes are well fit by Lorentzians.

The properties of the experimental ensemble may be partitioned into probe molecule orientation and probe molecule environment. In our case the ensemble consists of randomly oriented but otherwise identical microcrystals. Thus, there is no averaging over environmental variables, only orientation.

Orientation averaging is done straightforwardly. Orientation dependent molecular properties (in this case the transition dipoles and internal electric fields) are written in a molecule based Cartesian coordinate system. Unit vectors that specify laser polarization and the direction of the applied electric field are written in a Cartesian laboratory frame that is related to the molecular frame by an Euler rotation. At a given Euler rotation, the shift in transition energy is calculated using one of the models described below and intensity weight for this shift is calculated by multiplying the square of the dot product of the burn polarization and transition dipole times the square of the dot product of read polarization and transition dipole. By stepping through a grid of angles that cover all possible Euler rotations relating the laboratory and molecular frames (8000 is adequate in most cases), a stick spectrum of frequency shifts and intensities is generated. Convolution of this stick spectrum with the zero applied field hole profile then gives the calculated profile.

A local field tensor relates the electric field at the probe molecule generated by the externally applied field to the laboratory field. To the extent that this tensor is isotropic, this simply amounts to a linear scaling of the parameters of a given model. In these comparisons we have in all cases used a local field tensor that is 0.78 times the identity.[1]

PROBE MOLECULE RESPONSE

Classical Model

At a classical level the shift of transition energy with external electric field can be written

$$\Delta\nu = -\mathbf{E}\cdot\Delta\mu - \frac{1}{2}\mathbf{E}\cdot\Delta\alpha\cdot\mathbf{E} - \ldots$$

Equation 1

where $\Delta\mu$ is the difference between the excited and ground state dipole moments and $\Delta\alpha$ is the difference between excited and ground state polarizabilities. In low symmetry or disordered environments the observed shift of transition energy with external field

almost always depends linearly on field strength, even for centrosymmetric probe molecules. This is because the internal electric fields from neighboring molecules (of order 10^6-10^7 V/cm) is large compared to typical laboratory fields (of order 10^3-10^5 V/cm), in which case the dependence of the induced moment on applied field strength is too small to be observed. To make this point more clearly, we write the total electric field at the molecule as a sum of internal and external fields $\mathbf{E} = \mathbf{E}_{int} + \mathbf{E}_{loc}$ where the internal electric field $\mathbf{E}_{int}$, is the electric field produced by the charge distributions in the surrounding molecules and the local electric field $\mathbf{E}_{loc}$ is the field produced at the probe molecule by the externally applied field. Then, for a centrosymmetric molecule

$$\begin{aligned}\Delta\nu &= -\frac{1}{2}\mathbf{E}\cdot\Delta\alpha\cdot\mathbf{E} - \ldots \\ &= -\frac{1}{2}(\mathbf{E}_{int}+\mathbf{E}_{loc})\cdot\Delta\alpha\cdot(\mathbf{E}_{int}+\mathbf{E}_{loc}) - \ldots \\ &= -\frac{1}{2}\mathbf{E}_{int}\cdot\Delta\alpha\cdot\mathbf{E}_{int} - \mathbf{E}_{loc}\cdot\Delta\alpha\cdot\mathbf{E}_{int} - \frac{1}{2}\mathbf{E}_{loc}\cdot\Delta\alpha\cdot\mathbf{E}_{loc} - \ldots\end{aligned}$$

Equation 2

In the last line of Equation 2 the first term is a constant contribution to the overall solvent shift. The second term may be viewed as the interaction between the laboratory field and the moment induced by the internal field and the third term may be viewed as the interaction between the laboratory field and the moment induced by the laboratory field. Clearly, if $\mathbf{E}_{int} >> \mathbf{E}_{loc}$ the second term will dominate and the shift will appear to be given by $-\mathbf{E}_{loc}\cdot\Delta\mu_{ind}$ where $\Delta\mu_{ind} = \Delta\alpha\cdot\mathbf{E}_{int}$. Since this simple formula is capable of giving an empirical account of a large number of experiments, it is widely used to fit experimentally measured Stark profiles for randomly ordered ensembles. However, the value of $\Delta\mu_{ind}$ can be strongly affected by the internal electric field in a way that, given the lack of experimentally measured $\Delta\alpha$ tensors and the difficulties in observing the quadratic contributions to the shift, is at best poorly described at this classical level. This seriously compromises the usefulness of this approach.

Quantum Mechanical Models

In the LCAO-MO scheme with the zero-differential-overlap approximation, a quantum mechanical description of the effect of an external electric field on the transition energy of a neutral molecule begins with the 1-electron Hamiltonian

$$H_e = H_0 - e\sum_{i=atoms}\phi_i$$

Equation 3

where H_0 includes everything except the electrostatic perturbation of the conjugated system, e is the magnitude of the electronic charge, and ϕ_i is the potential at conjugated atom i (located at $\mathbf{r}_i$). The potentials ϕ_i consist of the sum of contributions from the charge distributions in surrounding molecules and $\mathbf{r}_i\cdot\mathbf{E}_{loc}$ from the externally applied field. Characterization of the local electrostatic environment depends on how the

contribution of the surrounding molecules is treated. We have used two models which we have labeled molecular resolution and atomic resolution.

Molecular Resolution

As a first approximation we can assume that the electrostatic potential generated at the probe by the charge distributions of the surrounding molecules can be approximated by a homogeneous electric field $\mathbf{E}_{int}$ so that

$$H_e = H_0 - e \sum_{i=atoms} (\mathbf{r}_i \cdot \mathbf{E}_{int} + \mathbf{r}_i \cdot \mathbf{E}_{loc})$$
$$= H_0 - \hat{\mu} \cdot (\mathbf{E}_{int} + \mathbf{E}_{loc})$$

Equation 4

This is equivalent to treating the molecule as a point object. The rather idealized characterization of the probe molecule electrostatic environment that is obtained in this case gives the effective internal electric field at molecular resolution. In most cases the real internal electric field is extremely inhomogeneous on the scale of the probe molecule's dimensions, so that the experimentally determined value of $\mathbf{E}_{int}$ gives only a rough approximation to the real situation.

One point relating to the mechanics of using Equation 4 to calculate transition energy shifts deserves comment. H_0 determines estimates for the molecular eigenstates Ψ_n which may then be used to calculate expectation values for any operator, including dipole moment and polarizability. Thus, one way to proceed would be to calculate the ground and excited state dipole moments and polarizabilities and then use these values in Equation 1. In principle, this introduces further approximations since, in a given basis, substituting eigenstate dipoles $\mu_{n,n}$ and polarizabilities

$$\alpha_{n,n} = 2 \sum_{i \neq n} \frac{\langle n|\hat{\mu}|i\rangle\langle i|\hat{\mu}|n\rangle}{E_i - E_n}$$

Equation 5

into Equation 1 only treats the perturbation to second order. The worry is that, because of the large magnitude of the effective internal electric field, the difference between shifts calculated this way and those calculated by diagonalizing Equation 4 (equivalent to taking the expansion in Equation 1 to infinite order) will be significant.

We can get a clearer idea of what is involved here by looking at one of the simplest cases imaginable: ethylene treated by Hückel theory. In the normal Hückel treatment the LCAO-MO's are $\Phi_{1,2} = \frac{1}{\sqrt{2}}(\chi_a \pm \chi_b)$ where $\chi_{a,b}$ are 2p atomic orbitals

on carbons a and b, respectively. The molecular orbital energies are $\pm\beta$ where β is the Hückel resonance integral. There are only three singlet configurations which, in terms of orbital occupation and energy are the ground state, $\Phi_1(1)\Phi_1(2)$ with energy $-2|\beta|$, the HOMO→LUMO single excitation $[\Phi_1(1)\Phi_2(2) + \Phi_1(2)\Phi_2(1)]/\sqrt{2}$ with energy 0, and the HOMO→LUMO double excitation $\Phi_2(1)\Phi_2(2)$ with energy $2|\beta|$. In the zero-differential overlap approximation expectation values of coordinate in the atomic orbital basis just give the atom coordinates: that is $\langle\chi_{a,b}|\mathbf{r}|\chi_{a,b}\rangle = \mathbf{r}_{a,b}\delta(a,b)$ so $\mu_{1,1} = \mu_{2,2} = 0$ and $\mu_{1,2} = \mu_{2,3} = eR/\sqrt{2}$ where $R = |\mathbf{r}_a - \mathbf{r}_b|$ (our coordinate origin was put at the center of nuclear charge so we need only need to consider the electronic contribution). Thus, by Equation 5 the ground state polarizability is $\alpha_{1,1} = \dfrac{e^2R^2}{2|\beta|}$.

By Equation 1 an electric field directed along the internuclear axis shifts the ground state energy to

$$W_g = -2|\beta|\left(1 + \frac{e^2R^2E^2}{8\beta^2}\right)$$

Equation 6

The ground state energy calculated by exact diagonalization in the basis of the three singlet configurations is $W_g = -2|\beta|(1 + \frac{e^2R^2E^2}{4\beta^2})^{\frac{1}{2}} \cong -2|\beta|(1 + \frac{e^2R^2E^2}{8\beta^2})$ with correction terms to the approximate equality being of order $2|\beta|(\frac{e^2R^2E^2}{4\beta^2})^2$. At a field strength of 10^7 v/cm $|eRE| \cong 250$ cm^{-1} which means that the relative size of the difference between the perturbation expansion and exact diagonalization in this case is order 10^{-4}. This can safely be ignored.

Atomic Resolution

The second way to model the effect of an applied field is to simply use Equation 3. This is more fundamental and accommodates the extremely inhomogeneous molecular electric fields that are found in complex organic solids. Given an adequate LCAO-MO description of probe molecule excitation energy, this approach can quantitatively characterize the electrostatic potential at the level of atomic resolution.

In this treatment we do not assume that the electrostatic potential produced by the charge distributions in surrounding molecules are equivalent to a homogeneous electric field. That is, we use the 1-electron Hamiltonian given above as Equation 3 and write the potential at conjugated atom i as a sum of contributions from the surroundings and the laboratory field $\phi_i = \phi_i' + \mathbf{r}_i \cdot \mathbf{E}_{loc}$. We have already commented on the fact that inhomogeneous electric fields are easily and naturally treated in this more fundamental approach. This site energy method is not only conceptually simpler and more general, it

also involves less computational effort. To demonstrate the operational simplicity of this method, we can again look at the extremely simple case of the Hückel theory treatment of ethylene in a homogeneous electric field.

For a homogeneous electric field directed along the internuclear axis the relative potentials at the two conjugated atoms are $\phi_{a,b} = \pm\frac{eRE}{2}$. This gives molecular orbital energies $W_{1,2} = \pm\left(\beta^2 + (eRE/2)^2\right)^{\frac{1}{2}}$ which means that the ground state energy is

$$W_g = -2\left(\beta^2 + (eRE/2)^2\right)^{\frac{1}{2}}$$
$$\cong -2|\beta|\left(1 + \frac{e^2R^2E^2}{8\beta^2}\right)$$

Equation 7

which is exactly the energy obtained in a sum-over-states calculation that included *all* singlet configurations. While the difference in computational overhead is relatively small in the case of two conjugated atoms, it becomes significant for larger systems.

COMPARISON OF THE MODELS

To make the preceding sections as concrete and instructive as possible, we will apply each of the analysis schemes to what for us has been a watershed data set: photochemical hole burning Stark effect measurements for octatetraene in polycrystalline n-hexane.[2] and n-heptane. These were the measurements that first taught us the importance of local structure and intermolecular perturbation and inspired us to try to develop a quantitative microscopic mapping of electrostatic potential.

Since the object here is to compare different analysis schemes rather than give the final and definitive analysis of these data, we address two tiny subsets of the total number of measured profiles. For the n-hexane host we chose 6 representative scans for a hole burned at 28743 cm^{-1} (3 with burning and reading laser polarizations parallel to the Stark field and 3 with burning and reading laser polarizations perpendicular to the Stark field): for the n-heptane hose we chose 2 representative scans for a hole burned at 28778.4 cm^{-1} (1 with burning and reading laser polarizations parallel to the Stark field and 1 with burning and reading laser polarizations perpendicular to the Stark field). All of these Stark scans were preceded and followed by a scan at zero applied field to determine the width of the Lorentzian profile and to verify that scanning had not changed the profile.

Classical Fit

Protocols for fitting measured Stark profiles by Equation 1 have been discussed elsewhere, as has intensity weighting for 1-, 2- and 3-dimensional conjugated networks.[3,4,5,6] Our own scheme is rather direct. Since the splitting or broadening of the measured profiles is linear in applied field strength, we follow the common practice and use only the first order term in Equation 1. Octatetraene is a 2-dimensional conjugated

network, so the ensemble averaging over the relative orientations of laboratory and molecular axes assumed that the transition dipole and $\Delta\mu$ are in the same plane. A linear baseline is added to the calculated profile whose center position is always adjusted to give best fit so up to four parameters can be varied: the magnitude of the dipole moment difference $\Delta\mu$, the angle between $\Delta\mu$ and the transition dipole θ, and two Gaussian distribution parameters for $\Delta\mu$. As is seen in Figure 1 and Figure 2 below, fits are already quantitative when it is assumed that $\Delta\mu$ is not distributed, so there is no reason in this case to consider anything beyond $\Delta\mu$ and θ.

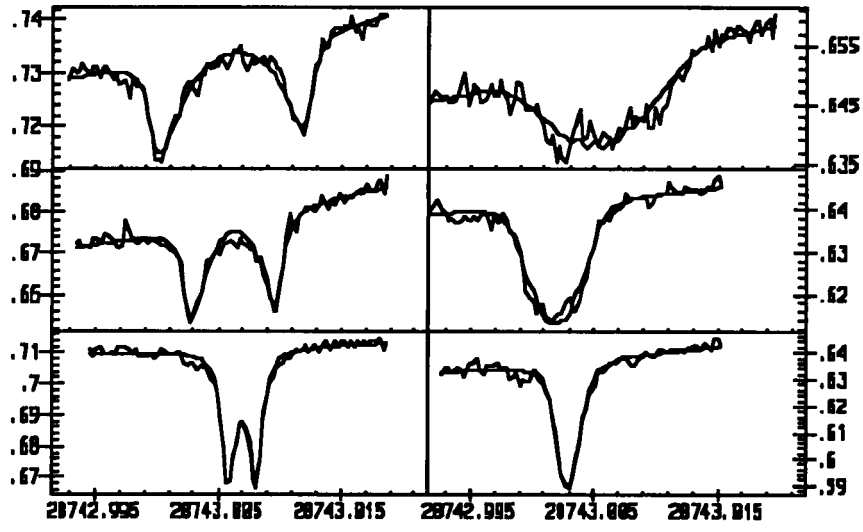

Figure 1 Comparison of fluorescence excitation Stark profiles measured for octatetraene in n-hexane (noisy lines)to those calculated from the linear term of Equation 1 (smooth lines). The left panel is for light polarized parallel to the applied field of 1380 V/cm (bottom), 4140 V/cm (center) and 6910 V/cm (top). The right panel is for light polarized perpendicular to the applied field of 1380 V/cm (bottom), 4140 V/cm (center) and 8290 V/cm (top).

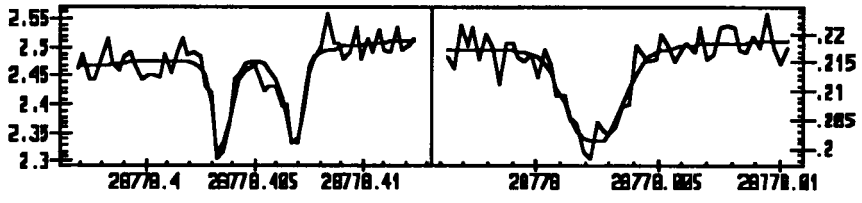

Figure 2 Comparison of fluorescence excitation Stark profiles measured for octatetraene in n-heptane (noisy lines) to those calculated from the linear term of

Equation 1 (smooth curves). The left panel is for light polarized parallel to the applied field of 5390 V/cm: the right panel is for light polarized perpendicular to the applied field of 5390 V/cm.

For the n-hexane host the best fit parameters are $\Delta\mu$=0.072 Debye, θ=19.2 degrees; for the n-heptane host the best fit parameters are $\Delta\mu$=0.028 Debye, θ=19.1 degrees. Despite the fact that this model reasonably reproduces the measured profiles, the information content of the best-fit parameter values is rather minimal. There is ambiguity in the meaning of the angle between $\Delta\mu$ and the transition dipole since the algebraic sign of θ is not determined. The fact that the induced dipole moment difference is larger in n-hexane than in n-heptane means that in some sense the internal field must also be larger, but quantitative conclusions require information about the $\Delta\alpha$ tensor. Further, it is important to realize that neglect of the second order term in Equation 1 is in general not reasonable. When the applied field is nearly normal to $\Delta\mu$, the second order term will be at least as important as the first order term. Since it is much more likely that two randomly chosen vectors will be nearly perpendicular rather than nearly parallel, neglect of the second order term can introduce considerable error into the calculated profiles which may be compensated for by distributing $\Delta\mu$. Because of this it is our view that there is little justification for ascribing any meaning to the distribution parameters obtained from this level of analysis.

Molecular Resolution Fit

At the molecular resolution level we assume that shifts in transition energies can be calculated from Equation 4. Since the LCAO-MO approach has advantages when it comes to assigning charges to atoms, this is what we use. What remains is to further specify the Hamiltonian and the basis set.

How Many States?

For quantum mechanical calculations in a finite basis set one quick answer to this question is "as many as possible". This is not really correct since we know that a few good states, for example, the relevant ground and excited state molecular eigenstates, are far better than a lot of states that have only a very little overlap with these eigenstates.

In our initial molecular resolution level analysis of octatetraene in n-hexane[2], we restricted the basis to the 1^1A_g ground state, and the 2^1A_g and 1^1B_u excited states. To come as close as possible to a molecular resolution level analysis in a truncated molecular eigenstate basis, we used experimentally measured instead of calculated excitation energies, but had to resort to theory[7]for the transition dipoles. Part of the rationale for such severe truncation was the small energy difference between the 2^1A_g and 1^1B_u excited states and the fact that the dipole matrix element between these two states is symmetry allowed.

Soos and Ramasesha[7] have published energies and dipole moment matrix elements for the first 16 π-electron states of octatetraene as obtained from a very high

level calculation. These results can be used to determine the degree to which this basis set could be truncated without significantly degrading the accuracy of Stark shifts calculated with Equation 4. This exercise is sometimes referred to as determining the "essential states".

Soos and Ramesesha's 16 states can be rearranged in order of their contribution to the sum-over-states polarizability of either the 1^1A_g ground state or the 2^1A_g excited state. This gives the ordering of states summarized in Table 1.

Table 1 Octatetraene π-electron states from reference 7 ordered according to their contribution to 1^1A_g or 2^1A_g state polarizabilities.

Number	State	Energy (cm^{-1})	Number	State	Energy (cm^{-1})
1	2^1A_g	30450	9	6^1B_u	80720
2	3^1B_u	60410	10	4^1B_u	71390
3	1^1A_g	0	11	5^1A_g	58650
4	1^1B_u	36790	12	8^1A_g	76060
5	2^1B_u	57120	13	7^1A_g	69320
6	8^1B_u	87310	14	4^1A_g	48400
7	5^1B_u	77080	15	3^1A_g	43050
8	7^1B_u	82210	16	6^1A_g	62620

As would be expected on the basis of the discussion in **Molecular Resolution**, the polarizability tensor elements calculated from the sum-over-states states formula and those derived by dividing the energy shift obtained by exact diagonalization by $\frac{1}{2}E_aE_b$ where $a,b = \{x,y,z\}$ are very nearly identical. Figure 3 summarizes how the calculated polarizability difference between the 2^1A_g and 1^1A_g states depends on the number of basis states. In Figure 3 the angle is the angle between the axis of smallest in-plane polarizability difference and the molecular z-axis so that an angle of 90^0 would correspond to the axis of largest in-plane polarizability being parallel to the polyene chain axis.

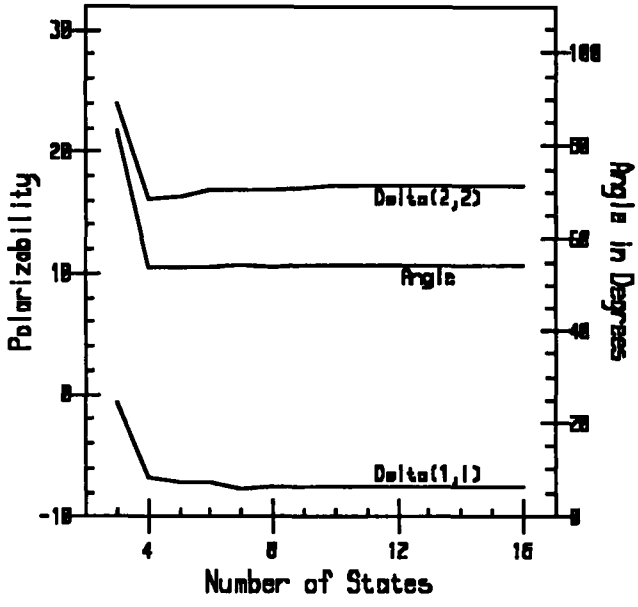

Figure 3 Octatetraene 2^1A_g state polarizability minus 1^1A_g state polarizability versus the number of states in the truncated basis.

The behavior of the calculated polarizability of the individual states is completely analogous in that the values calculated with the first four states differ very little from those obtained in the 16 state limit. Thus, our molecular resolution model for octatetraene would be significantly improved by adding the 3^1B_u state, and, to the extent that the basis states reasonably approximate molecular eigenstates, there is little incentive to go further.

Hamiltonian and Basis

We have previously described a simple quantum mechanical model called the HSS model that quantitatively reproduces the 2^1A_g and 1^1B_u 0-0 excitation energies measured for low temperature n-alkane solutions of linear polyenes with 3 through 8 conjugated double bonds.[8] Because it contains a judicious choice of empirical elements, it is both extremely simple and much more accurate than more elaborate calculations. In the initial formulation of this model the focus was on excitation energies only. Three minor changes are needed in order to use it to calculate dipole moment matrix elements. First, the HOMO→LUMO+1 configuration has to be changed to the energetically degenerate $\frac{1}{\sqrt{2}}((\text{HOMO} \rightarrow \text{LUMO}+1)+(\text{HOMO}-1 \rightarrow \text{LUMO}))$ configuration. Second, the 3^1B_u state is added to the basis. Third, the molecular geometry must be specified. We use single and double bond lengths 1.451 Å and 1.332 Å, respectively, with all C=C-C bond angles equal to 125^0. Cartesian coordinate axes are chosen such that the molecule

lies in the *yz* plane, the origin is at the inversion center and the *z*-axis goes through the bond centers.

Table 2 compares the sum-over-states polarizability tensor elements calculated with this model to those computed with the 16 π-electron states and associated dipole matrix elements reported by Soos and Ramasesha[7].

Table 2 Comparison of sum-over-states polarizability tensor elements (in $\mathring{A}^3$) calculated with the HSS model to those calculated from the energies and dipole elements given in ref 7.

Method	α_{yy}	α_{yz}	α_{zz}
1^1A_g (states and dipoles from ref. 7)	2.53	5.33	20.24
1^1A_g (HSS)	0.87	-4.22	20.37
2^1A_g (states and dipoles from ref 7)	3.40	-6.39	28.93
2^1A_g (HSS)	2.81	-13.55	65.39

The only significant difference is for the chain axis component of the 2^1A_g state polarizability. Which calculation gives the better estimate remains to be determined.

The final piece of information that is needed before orientationally averaged Stark profiles can be calculated is the direction of the $1^1A_g \rightarrow 2^1A_g$ transition dipole in this molecular axis set. Since our holes are burned into the 0-0 band, vibronic coupling considerations are not relevant: intensity is solely derived from the fact that the molecule in a non-centrosymmetric potential. Calculations of the derivatives of the components of this transition dipole on site energy[9] show that the derivatives for the *z* component are at least an order of magnitude larger than the *x* or *y* components. Thus, in our analysis we have assumed that the 0-0 band is *z* polarized.

Results

In fitting data with Equation 4, the two variable parameters are the *y* and *z* components of the internal electric field. However, because of the very large anisotropy, the *y* component is not well determined by these data. The fits obtained by varying only the z component are shown in Figure 4 and Figure 5.

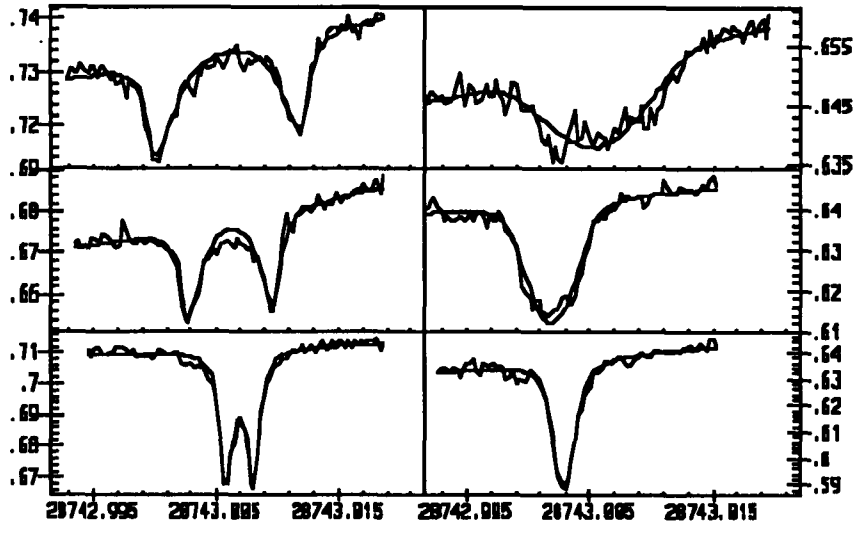

Figure 4 Comparison of fluorescence excitation Stark profiles measured for octatetraene in n-hexane (noisy lines)to those calculated from Equation 4 (smooth lines) for internal field components E_y=0 and Ez=355,000 V/cm. The left panel is for light polarized parallel to the applied field of 1380 V/cm (bottom), 4140 V/cm (center) and 6910 V/cm (top). The right panel is for light polarized perpendicular to the applied field of 1380 V/cm (bottom), 4140 V/cm (center) and 8290 V/cm (top).

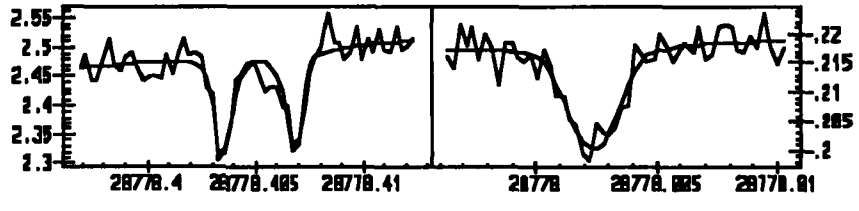

Figure 5 Comparison of fluorescence excitation Stark profiles measured for octatetraene in n-heptane (noisy lines) to those calculated from Equation 4 (smooth lines) for internal field components E_y=0 and Ez=136,000 V/cm. The left panel is for light polarized parallel to the applied field of 5390 V/cm: the right panel is for light polarized perpendicular to the applied field of 5390 V/cm.

As is seen in Figure 4 and Figure 5, with one rather than two adjustable parameters this model gives as good an accounting of the data as does the classical model. Even though only one component of the internal field is significant, the explicit quantum mechanical model fixes both the magnitude of $\Delta\mu$ and the absolute sense of the angle θ.

Atomic Resolution (HSSISS)

In this case, instead of using Equation 4 which assumes that the internal electric field is constant over the octatetraene molecule we use the more general Equation 3. The simple but accurate quantum mechanical model that was described above in the section titled Hamiltonian and Basis is based on Hückel theory which assumes that in the absence of external perturbation diagonal matrix elements of the effective 1-electron Hamiltonian in the atomic orbital basis are all equal ($\int \chi_i H \chi_i d\tau = \alpha$). To calculate the transition energy for an arbitrary set of potentials at the conjugated atoms ϕ_i, α for the i^{th} atom is changed to $\alpha + \phi_i$, otherwise the calculation is the same. There are two contributions to the potentials ϕi, $-e\mathbf{E}_{loc} \cdot \mathbf{r}_i$ from the externally applied field and ϕ_i^{int} from the charge distributions in the surrounding molecules.

Calculating a Stark profile in this completely microscopic approach involves three steps which have been described elsewhere.[10] First, the structure of the octatetraene site is determined by molecular mechanics. Second, the potentials at the octatetraene carbon atoms ϕ_i^{int} are calculated by summing over the charge distributions of all n-alkane molecules whose centers are within 100 Å of the octatetraene impurity. Then , third, the orientationally averaged Stark profile is calculated using the HSSISS model. There is only one variable parameter, the scaling factor for the n-alkane charge distribution. Given this number (which should be close to unity), the Stark profile for a given polarization in a given n-alkane is completely determined.

The molecular mechanics calculation that gives us the site structure exhibits a number of local minima (4 for n-hexane and 16 for n-heptane) so there are a number of different geometries that must be examined for each of the hosts. In all of the calculated structures there is little distortion of the n-alkane structure. That is, in all cases the octatetraene is in a vacancy created by removing one or two molecules from the n-alkane crystal and the positions of the atoms of the remaining n-alkane molecules deviate at most 0.01 Å from the positions they had in the original crystal. For each of geometries corresponding to one of these local minima, the n-alkane charge distribution scaling factor that best fits the measured profiles can be determined. This parameter must be the same for the n-hexane and n-heptane hosts and should not differ from unity by more than a factor of four. There is only one pair of structures out of the 64 for which this condition is met, a hexane site where the octatetraene occupies a molecule vacancy created by removing two adjacent host molecules related by a *c* translation and a heptane site where the octatetraene is in a vacancy created by removing two adjacent host molecules related by a *b* translation. In the hexane site the potentials at the octatetraene carbons in $cm^{-1}/|e|$ are: 139, 146, 246, 245, 213, 148, 172, and 174. In the heptane site the potentials at the octatetraene carbons in $cm^{-1}/|e|$ are: 300, 159, 161, 159, 210, 164, 213, 135. This will be described in detail in another paper.[9] The important point here is that, as can be seen in Figure 6 and in Figure 7 this atomic resolution model with only one variable parameter fits the measurements in *both* hosts reasonably well.

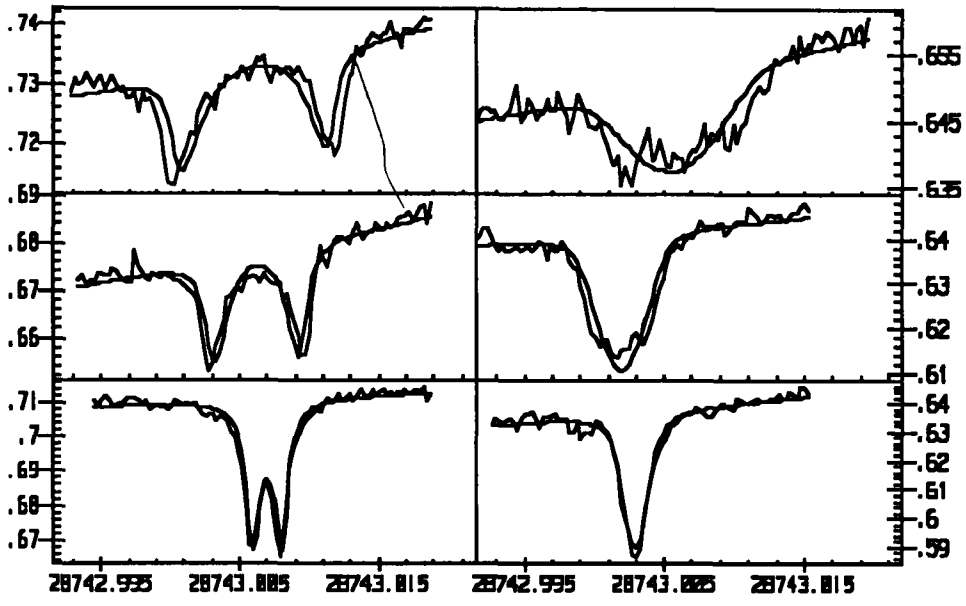

Figure 6 Comparison of fluorescence excitation Stark profiles measured for octatetraene in n-hexane (noisy lines)to those calculated from the HSSISS model with the n-alkane charge distribution scaled by the factor 1.20 (smooth lines). The left panel is for light polarized parallel to the applied field of 1380 V/cm (bottom), 4140 V/cm (center) and 6910 V/cm (top). The right panel is for light polarized perpendicular to the applied field of 1380 V/cm (bottom), 4140 V/cm (center) and 8290 V/cm (top).

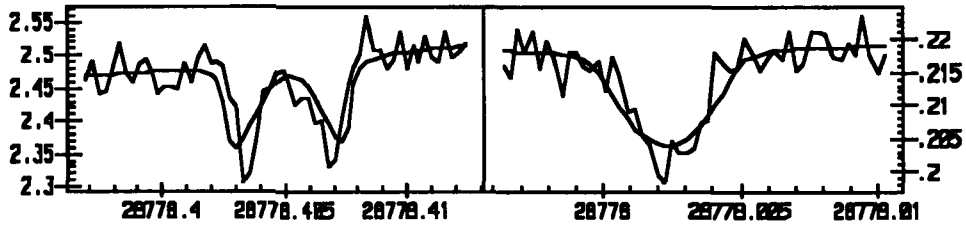

Figure 7 Comparison of fluorescence excitation Stark profiles measured for octatetraene in n-heptane (noisy lines) to those calculated from the HSSISS model with the n-alkane charge distribution scaled by the factor 1.20 (smooth lines). The left panel is for light polarized parallel to the applied field of 5390 V/cm: the right panel is for light polarized perpendicular to the applied field of 5390 V/cm.

The deviations between the calculated and measured profiles are discernibly larger in this case than for the classical or molecular resolution fits. This more likely a consequence of our using a scalar local field factor rather that tensors calculated as described in reference 10 and using a single idealized octatetraene geometry in the HSS calculations rather than the geometries found in the molecular mechanics calculations. A more careful analysis where these approximations are not made is in progress. While

there is good reason to think that this more careful treatment will do an even better job of quantitatively accounting for the measured profiles, we shouldn't minimize the significance of what has already been accomplished, a quantitative accounting for Stark splittings that differ by a factor of three for the same chromophore in two hosts that are nearly identical in their macroscopic properties.

There are at least three advantages to this kind of analysis. First, it is faithful to the real microscopic situation where the internal electrostatic field is decidedly *not* constant over the dimensions of the probe molecule. Second, it shifts our attention from something that we already understand reasonably well (how excitation energy depends on site potential in a simple conjugated molecule) to something that we know much less about (how to model the charge distribution of an organic molecule in the condensed phase). Third, it greatly increases the information content of these kinds of Stark experiments (in this case giving us a general quantitative model for the charge distribution in an n-alkane in a crystal and a detailed picture of the site structure in the n-hexane and n-heptane hosts).

CONCLUSION

Simple quantum mechanical models that reasonably describe the effect that changing the potential at a conjugated atom has on transition energy can be combined with structures derived from molecular mechanics calculations to compute Stark shifts without making the unjustified assumptions involved in classical and point multipole treatments. In combination with photochemical hole burning Stark measurements, these kinds of models lead to an atomic resolution mapping of intermolecular electrostatic potential.

ACKNOWLEDGMENTS

This research is supported by the NSF under grant number CHE-9417103. BEK thanks the DFG (Deutsche Forschungsgemeinschaft) for supporting a visit to Bayreuth, Dietrich Haarer and Josef Friedrich for providing an ideal environment for working through these ideas, and Bob Silbey, who caught a potentially embarassing mistake having to do with permutation symmetry.

REFERENCES

[1] P. Geissinger, B.E. Kohler and J.C. Woehl, J. Phys. Chem. **99**, 16527 (1995). Derivation of the factor 0.78 is described in footnote 18.

[2] G. Gradl, B.E. Kohler and C. Westerfield, J. Chem. Phys. **97**, 6064 (1992).

[3] V.D. Samoilenko, N.V. Rasumova and R.I. Personov, Opt. Spectrosc. (USSR) **52**, 346 (1982).

[4] M. Maier, Appl. Phys. B **41**, 73 (1986).

[5] A.J. Meixner, A. Renn, S.E. Bucher and U.P. Wild, J. Phys. Chem. **90**, 6777 (1986).

[6] L. Kador, D. Haarer and R.I. Personov, J. Chem. Phys. **86**, 5300 (1987).

[7] Z.G. Soos and S. Ramasesha, J. Chem. Phys. **90**, 1067 (1989).

[8] B.E. Kohler, J. Chem. Phys. **93**, 5838 (1990).

[9] Paper in progress to be submitted to J. Chem. Phys.

[10] B.E.Kohler and J.C. Woehl J. Chem Phys. **102**, 7773 (1995).